2021 43rd Annual International Conference of the
IEEE Engineering in Medicine & Biology Society (EMBC)
Oct 31 - Nov 4, 2021. Virtual Conference

Electrode Spacing and Current Distribution in Electrical Stimulation of Peripheral Nerve: A Computational Modeling Study using Realistic Nerve Models

Jinze Du[1], *Student Member, IEEE,* Andres Morales[2], *Student Member, IEEE,* Javad Paknahad[1], *Student Member, IEEE,* Pragya Kosta[3], *Member, IEEE,* Jean-Marie C. Bouteiller[2], *Senior Member, IEEE,* Eduardo Fernandez[4], *Member, IEEE,* and Gianluca Lazzi[1,2,3], *Fellow, IEEE*

Abstract— **Electrical stimulation of peripheral nerves has long been used and proven effective in restoring function caused by disease or injury. Accurate placement of electrodes is often critical to properly excite the nerve and yield the desired outcome. Computational modeling is becoming an important tool that can guide the rapid development and optimization of such implantable neural stimulation devices. Here, we developed a heterogeneous very high-resolution computational model of a realistic peripheral nerve stimulated by a current source through cuff electrodes. We then calculated the current distribution inside the nerve and investigated the effect of electrodes spacing on current penetration. In the present study, we first describe model implementation and calibration; we then detail the methodology we use to calculate current distribution and apply it to characterize the effect of electrodes distance on current penetration. Our computational results indicate that when the source and return cuff electrodes are placed close to each other, the penetration depth in the nerve is shallower than the cases in which the electrode distance is larger. This study outlines the utility of the proposed computational methods and anatomically correct high-resolution models in guiding and optimizing experimental nerve stimulation protocols.**

I. INTRODUCTION

Electrical stimulation of peripheral nerve is used for various applications including pain treatment [1], restoration of motor functions following spinal cord injury or stroke [2, 3], and treatment of epilepsy by vagus nerve stimulation [4]. Different electrode designs have been developed for efficient nerve stimulation, such as spiral electrodes [5], cuff electrodes [6], intrafascicular interfaces with thin wires [7, 8], and silicon probes [9, 10]. Cuff electrodes are amongst the most widely used electrodes for peripheral nerves since they have several advantages compared to others: 1) they allow for the reduction of input current intensity, and thus, minimize the possibility of nerve damage, 2) they allow for correct positioning of electrode leads to minimize mechanical distortion and damage, and 3) provide selective stimulation of nerve fascicles.

There have been numerous neurophysiological studies designed to evaluate the effect of electrode position on neural excitation. Early studies by Simmons and Glattke [11] and Walloch and Cowden [12] demonstrated that electrical stimulation is more efficient in exciting nerve fibres than Scala tympani stimulation when electrodes were placed directly into the nerve. Shepherd et al. [13] found that the optimal electrode position for auditory nerve excitation results in significant threshold reduction. However, few studies focused on parametric assessment of the effectiveness of peripheral nerve stimulation using very-large scale, anatomically correct, peripheral nerve models.

In this paper, we have utilized convolutional neural network segmentations of nerve cross sectional images along with a multi-scale, computational model of field distribution to study the effect of cuff electrode positions on peripheral nerve stimulation. Our multi-scale computational modeling platform is based on the Admittance Method (AM) [14] to predict the electric fields generated inside peripheral nerve tissue. Peripheral nerve tissue is represented by a heterogeneous very high-resolution nerve model that is based on segmented cross-sectional images of rat sciatic nerve and includes fine details such as axons and myelin. Using AM computed electric field values and current distribution inside the nerve, we investigated the effect of the distance that separates the source and return cuff electrodes on the internal current distribution, which provide a basis for application-specific electrode design.

II. METHODS

A. Building Nerve Model using CNN Segmentation of Peripheral Nerve Cross-sectional Images

Due to the complexity and the densely populated inner nerve structures, to the best of our knowledge, none of the currently used computational models of peripheral nerve stimulation are based on realistic very high resolution model replicated from true peripheral nerves [15]. In

*This work was supported by the NIBIB of the National Institute of Health Grant No. 5R01EB029271, and an unrestricted grant to the Department of Ophthalmology from Research to Prevent Blindness, New York, NY.

[1] J. Du and J. Paknahad are with the Department of Electrical Engineering, University of Southern California, Los Angeles, CA 90089, USA.

[2] A. Morales and J-M Bouteiller are with the Department of Biomedical Engineering, University of Southern California, Los Angeles, CA 90089, USA.

[3] P. Kosta is with the Institute for Technology and Medical Systems Innovation (ITEMS), Keck School of Medicine, University of Southern California, Los Angeles, CA 90089, USA.

[4] E. Fernandez is with the Institute of Bioengineering, University Miguel Hernandez, Elche and CIBER-BBN, Spain.

[1,2,3] G. Lazzi is with the Department of Biomedical Engineering, Department of Electrical Engineering and ITEMS, University of Southern California, Los Angeles, CA 90089, USA.

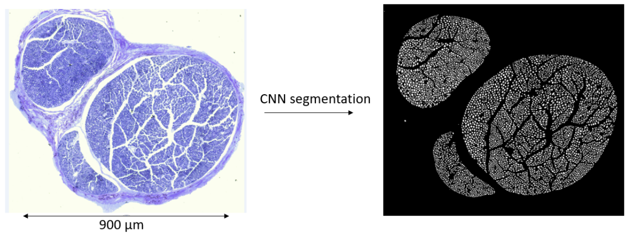

Fig. 1. CNN segmentation of cross-sectional image of peripheral nerve. (a) a cross-sectional image of rat sciatic nerve, (b) segmented image of nerve cross-section containing multiple fascicles populated by axons of various radii and myelin(grey represents myelin and white represents axon).

fact, most of the studies use either simplified nerve model with homogeneous fascicles or heterogeneous fascicles populated by axons with artificial radii and locations [16–19]. Thus, we constructed a peripheral nerve model using high-resolution cross-sectional image of a real peripheral nerve. To accomplish this, we utilized a confocal image of rat sciatic nerve and performed image segmentation to highlight axons and myelin. Image segmentation is performed using AxonDeepSeg, an open source easily trained convolutional neural network (CNN) described in [20]. The confocal image and the resulting segmented image are shown in Fig. 1. Next, the segmented cross-sectional image is discretized and extruded to build the pseudo-3D length of nerve for electrical stimulation modeling.

B. Model Building and Admittance Method

The multi-scale model considered for peripheral nerve stimulation consists of two main components: the segmented nerve model and the model of cuff electrode. The cuff electrodes are modeled based on the cuff electrode design from typical commercial cuff electrode, with 3 metal contact wires in each cuff electrode. Only the metal contact part of the electrode is modeled while the other non-conductive elements that are not in touch with the tissue, such as the surrounding insulation layer, are discarded since they do not impact the current distribution in the tissue. Three simulation models with different electrode positions are considered in this study as visualized in Fig. 2. The size of the model is 300x300x550 voxels in x, y, z dimensions and the resolution is 8 µm in all three dimensions. The model is discretized in cubic voxels and each voxel is represented by a unique material index. The material properties of the nerve model are taken from [21, 22] and described in Table 1.

The multi-resolution admittance method (AM) [14] is used to compute electric field values at each node of the computation grid [23–26]. AM defines a matrix describing the admittance (G), or resistance, throughout the model. The resistance of each node is defined by the diagonal components of the matrix, while the surrounding values define the resistances between nodes, producing a sparse, diagonal matrix. The admittance values are computed using the conductivity and the distance between nodes in the x, y,

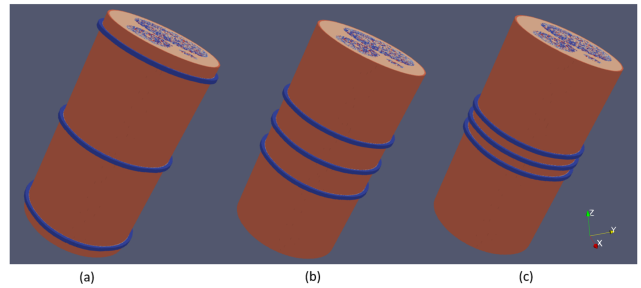

Fig. 2. Simulation models consisting of the nerve and three cuff electrodes (shown in blue color). Source electrodes are at the top, return electrodes are at the bottom and floating electrodes are in the middle. Distances between source and return electrodes are: (a) 4 mm, (b) 2 mm, (c) 1 mm.

TABLE I
TISSUE PROPERTIES

Tissue Type	Conductivity (σ_x, σ_y, σ_z)S/m
Perineurium	(0.01, 0.01, 0.01)
Myelination	(2×10^{-4}, 5×10^{-9}, 5×10^{-9})
Intracellular space	(0.91, 0.91, 0.91)
Extracellular space	(0.33, 0.33, 0.33)

and z directions, as described in Equation 1.

$$g_x^{i,j,k} = \sigma_x^{i,j,k} \frac{\Delta y \Delta z}{\Delta x} \tag{1}$$

A current vector (I) is defined with current values applied to whichever nodes contain a source. A voltage vector (V) can then be solved for using G and I in Equation 2. A multi-threaded Python program using a biconjugate gradient algorithm is developed to construct the matrices and solve the matrix equation with accelerated speed.

$$GV = I \tag{2}$$

A 3D multi-resolution meshing algorithm is executed prior to the field simulations in order to reduce the complexity of the problem without impacting the accuracy of the solution. In this, a high level of details and fine resolution is maintained near the nerve periphery, in locations proximal to the contact electrode, and the voxel size is increased further away from nerve periphery where fine resolution is

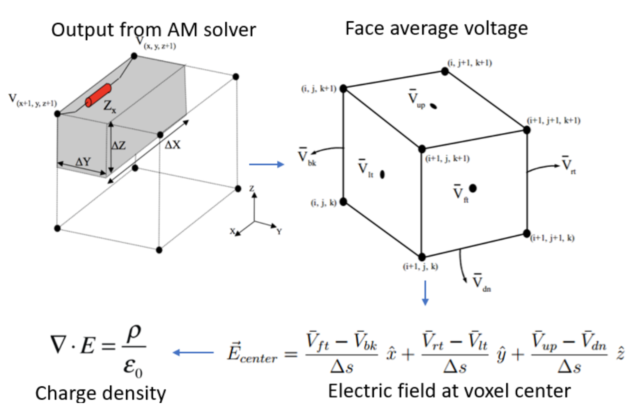

Fig. 3. Interpolation process to get current density value from Admittance Method output, Δs represents unit voxel size.

unnecessary. Therefore, along the center of the nerve bundle, the resolution would be coarser, whereas along the periphery of the nerve (i.e. closer to the electrodes and fascicle edges), the resolution would remain fine. In this way, the number of nodes and edges are decreased and the computational complexity of the system is reduced.

C. Current Density: Interpolation of Voltage Values

AM simulations provide voltage values at every node of the model. In our multi-resolution scheme, network nodes are located at the vertices of voxels. Because conductivity value is considered constant inside each voxel, trilinear interpolation is used to calculate the voltage at arbitrary points inside a voxel from the values at its vertices. Once voltage values have been interpolated back to unit voxel, electric field, charge density and current density could be calculated at any point in the model. The entire interpolation process is depicted in Fig. 3.

III. RESULTS

A. Current Distribution inside the Nerve

A Python program is developed to interpolate AM computed electric field and to compute current density distributions inside all three simulation models. As an example, the current density distribution inside the nerve for simulation model with 4 mm electrode spacing is shown in Fig. 4. A 3D perspective view of the simulation model is shown on the top panel of the figure. In the bottom panels, the current density distribution inside the nerve is plotted at three different XY-slices, each located at three electrodes positions. Current distribution on XY-slices corresponding to source and return electrode locations (Fig. 4(a) and (c)) demonstrate that the current density values are higher near the nerve periphery and near the edges of fascicles which are close to electrodes. Further, we can see the hot spots at the edge of fiber fascicles in the slices with electrodes. Conversely, for the XY-slice located at the non-functional floating electrode (Fig. 4(b)), far from source and return electrodes, inside the fiber fascicles there is higher current flowing inside the axon intracellular space due to its low resistivity. The axon intracellular space works as a conductive channel that can deliver current from

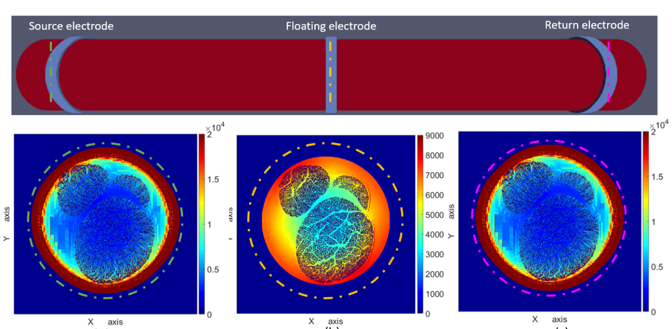

Fig. 4. Current density distribution in 4 mm model configuration, the xy cross-sectional layers are plotted on different slices: (a) on the source electrode level, (b) on the floating electrode level, (c) on the return electrode level. Unit: mA/m^2.

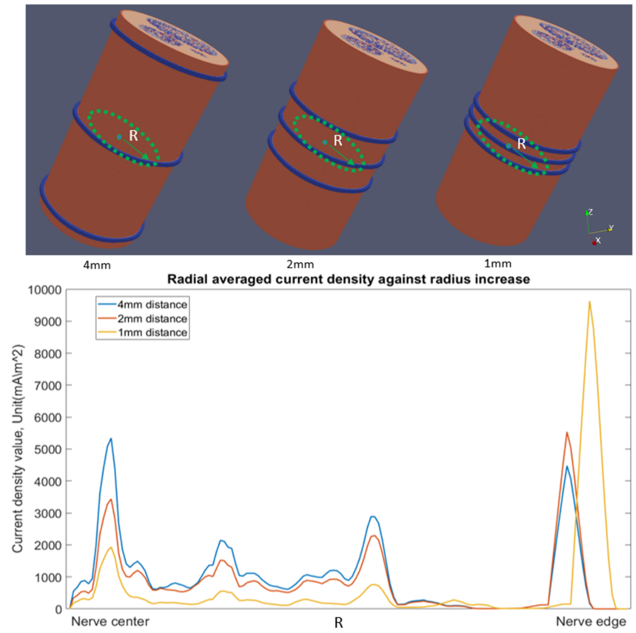

Fig. 5. Line plot of radial average values extracted from slices with floating electrode from all three models

source electrode to return electrode throughout entire nerve. In comparison to extracellular space, a lower current flows through the extracellular space.

B. Current Penetration Depth and Electrode Separation

All three simulation models (with 4 mm, 2 mm and 1 mm electrodes spacing) consider a stimulation level of 100 μA current amplitude. Every other detail of these models is ensured to be the same except the electrodes locations. For all three simulation models, we computed the radial average values of the current density on the floating electrode slices. Fig. 5 presents the plots of these radial average current density values with respect to the radial distance, R, ranging from the nerve center to the nerve edge. Results presented in Fig. 5 suggest that when the source and return electrodes are placed at 1 mm separation distance, the current flowing in the center of the nerve is significantly lower than that of 2 mm and 4 mm separation distances. Therefore, these results suggest that when the source and return electrodes are placed too close to each other, current penetration into the nerve center is less compared to the cases when source and return electrodes are separated farther. In addition, the current distribution peak for the 1 mm electrode distance setup is near the nerve bundle edge, which implies that the current is not flowing deep enough into the nerve center to recuit a large number of fibers. Rather current is flowing along the nerve edge area directly from the source electrode to the return electrode without entering deep into the center. Finally, the curves in Fig. 5 suggest that the heterogeneity of the nerve model significantly affects the current distribution inside the nerve. Therefore, realistic heterogeneous peripheral nerve models are essential for the analysis and design of peripheral neurostimulation electrodes.

IV. DISCUSSION

A computational study using the Admittance Method multi-scale computational platform was conducted to further our understanding of the effect of electrical stimulation site in the peripheral nerve electrical stimulation. We first performed the image segmentation of nerve cross-sectional images using convolutional neural network and then built realistic peripheral nerve models from the segmentation results. We also developed realistic cuff electrode models with different separation distances between electrodes. We found that the current distribution values around the nerve center are lower when the source electrode and return electrode are placed in a closer vicinity. Our results suggest that the accurate, high-resolution anatomical features of the peripheral nerve significantly affect the current distribution inside the nerve. This suggests that a very high resolution and accurate model of the peripheral nerve plays a critical role in the design and optimization of neurostimulating electrodes. Besides implications on recruitment of target fibers, the significant variations due to the model heterogeneity have implications on the level of stimulation that are considered safe and do not induce axonal damage. Thus, with the proposed method and models, criteria for safe and effective peripheral neurostimulations can be established.

REFERENCES

[1] Richard L Weiner. "The future of peripheral nerve neurostimulation". In: *Neurological Research* 22.3 (2000), pp. 299–304.

[2] Richard B Stein, P Hunter Peckham, and Dejan Popović. *Neural prostheses: replacing motor function after disease or disability*. Oxford University Press, 1992.

[3] Warren M Grill and Robert F Kirsch. "Neuroprosthetic applications of electrical stimulation". In: *Assistive Technology* 12.1 (2000), pp. 6–20.

[4] MC Salinsky. "The Vagus Nerve Stimulation Study Group. A randomized controlled trial of chronic vagus nerve stimulation for treatment of medically intractable seizures". In: *Neurology* 45 (1995), pp. 224–230.

[5] James D Sweeney, David A Ksienski, and J Thomas Mortimer. "A nerve cuff technique for selective excitation of peripheral nerve trunk regions". In: *IEEE Transactions on Biomedical Engineering* 37.7 (1990), pp. 706–715.

[6] Jytte Overgaard Larsen et al. "Degeneration and regeneration in rabbit peripheral nerve with long-term nerve cuff electrode implant: a stereological study of myelinated and unmyelinated axons". In: *Acta neuropathologica* 96.4 (1998), pp. 365–378.

[7] BR Bowman, LL Baker, and RL Waters. "Positional feedback and electrical stimulation: an automated treatment for the hemiplegic wrist." In: *Archives of physical medicine and rehabilitation* 60.11 (1979), pp. 497–502.

[8] Timothy G McNaughton and Kenneth W Horch. "Metallized polymer fibers as leadwires and intrafascicular microelectrodes". In: *Journal of neuroscience methods* 70.1 (1996), pp. 103–107.

[9] Peter H Veltink et al. "A modeling study of nerve fascicle stimulation". In: *IEEE transactions on biomedical engineering* 36.7 (1989), pp. 683–692.

[10] Phillip W Barth, Sharon Lea Bernard, and James B Angell. "Flexible circuit and sensor arrays fabricated by monolithic silicon technology". In: *IEEE Transactions on electron devices* 32.7 (1985), pp. 1202–1205.

[11] F Blair Simmons and Theodore J Glattke. "Comparison of electrical and acoustical stimulation of the cat ear". In: *Annals of Otology, Rhinology & Laryngology* 81.5 (1972), pp. 731–738.

[12] Richard A Walloch and David A Cowden. "Placement of electrodes for excitation of the eighth nerve". In: *Archives of Otolaryngology* 100.1 (1974), pp. 19–23.

[13] RK Shepherd, S Hatsushika, and Graeme M Clark. "Electrical stimulation of the auditory nerve: the effect of electrode position on neural excitation". In: *Hearing research* 66.1 (1993), pp. 108–120.

[14] Carlos Cela et al. "A multiresolution admittance method for large-scale bioelectromagnetic interactions". PhD thesis. 2010.

[15] Eleanor V Goodall et al. "Modeling study of activation and propagation delays during stimulation of peripheral nerve fibers with a tripolar cuff electrode". In: *IEEE Transactions on Rehabilitation Engineering* 3.3 (1995), pp. 272–282.

[16] S Raspopovic, M Capogrosso, and S Micera. "A computational model for the stimulation of rat sciatic nerve using a transverse intrafascicular multichannel electrode". In: *IEEE Transactions on Neural Systems and Rehabilitation Engineering* 19.4 (2011), pp. 333–344.

[17] P Kosta et al. "Simulation-Based Optimization of Figure-of-Eight Coil Designs and Orientations for Magnetic Stimulation of Peripheral Nerve". In: *IEEE Transactions on Neural Systems and Rehabilitation Engineering* (2020).

[18] P Kosta, D J Warren, and G Lazzi. "Selective stimulation of rat sciatic nerve using an array of mm-size magnetic coils: a simulation study". In: *Healthcare technology letters* 6.3 (2019), pp. 70–75.

[19] A K RamRakhyani et al. "A μm-Scale Computational Model of Magnetic Neural Stimulation in Multifascicular Peripheral Nerves". In: *IEEE Transactions On Biomedical Engineering* 62.12 (2015), pp. 2837–2849.

[20] Aldo Zaimi et al. "AxonDeepSeg: automatic axon and myelin segmentation from microscopy data using convolutional neural networks". In: *Scientific reports* 8.1 (2018), pp. 1–11.

[21] Donald R McNeal. "Analysis of a model for excitation of myelinated nerve". In: *IEEE Transactions on Biomedical Engineering* 4 (1976), pp. 329–337.

[22] Christopher R Butson et al. "Selective neural activation in a histologically derived model of peripheral nerve". In: *Journal of neural engineering* 8.3 (2011), p. 036009.

[23] John Stang et al. "Recent Advances in Computational and Experimental Bioelectromagnetics for Neuroprosthetics". In: *2019 International Conference on Electromagnetics in Advanced Applications (ICEAA)*. 2019, pp. 1382–1382.

[24] Javad Paknahad et al. "Responsiveness of Retinal Ganglion Cells Through Frequency Modulation of Electrical Stimulation: A Computational Modeling Study*". In: *2020 42nd Annual International Conference of the IEEE Engineering in Medicine Biology Society (EMBC)*. 2020, pp. 3393–3398.

[25] Javad Paknahad et al. "Color and cellular selectivity of retinal ganglion cell subtypes through frequency modulation of electrical stimulation". In: *Scientific reports* 11.1 (2021), pp. 1–13.

[26] Javad Paknahad et al. "Targeted Stimulation of Retinal Ganglion Cells in Epiretinal Prostheses: A Multiscale Computational Study". In: *IEEE Transactions on Neural Systems and Rehabilitation Engineering* 28.11 (2020), pp. 2548–2556.